ACS APPLIED MATERIALS & INTERFACES

Research Article

www.acsami.org

Design of Single-Site Ti Embedded Highly Hydrophilic Silica Thin Films with Macro–Mesoporous Structures

Takashi Kamegawa, Yuki Masuda, Norihiko Suzuki, Yu Horiuchi, and Hiromi Yamashita*

Division of Materials and Manufacturing Science, Graduate School of Engineering, Osaka University, 2-1 Yamadaoka, Suita, Osaka 565-0871, Japan

Supporting Information

ABSTRACT: Single-site Ti-containing macroporous silica thin films with mesoporous frameworks were successfully prepared on quartz substrate with high transparency by using poly(methyl methacrylate) (PMMA) microspheres and organic surfactant as template of porous structures. The presence of mesoporous structure and the differences of macroporous structure of film surface were investigated by XRD and FE-SEM measurements. The local structure of Ti moieties embedded within silica matrixes were also confirmed by UV–vis investigations. It was found that the macroporous structure and the embedded single-site Ti moieties within mesoporous frameworks were quite effective for improvement of surface hydrophilicity, i.e., the water droplet was entirely spread on the film surface even before and after irradiation of UV light.

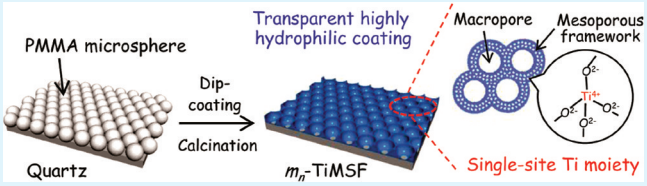

KEYWORDS: *single-site photocatalyst, transparent thin film, macropore, mesopore, surface hydrophilicity*

1. INTRODUCTION

Recently, the design and control of the ideal surface structure of thin films have attracted considerable attention because of their importance in promising applications in the fields of functional coatings, sensor devices, and the mimesis of natural products.[1−7] The unique surface structures have been designed by direct synthesis methods such as sol–gel, chemical vapor deposition (CVD), and plasma process as well as postsynthetic chemical treatments of thin films by acidic or basic solutions.[1−7] The usages of polymer microspheres as template materials, which are easily removable by heat treatment or solvent extraction, have also been made to control the architectures of thin films through bottom-up process.[8−10] The surface structure of thin films strongly affects the characteristics such as wettability, crystal growth and joining observed in a solid–liquid, solid–gas and solid–solid interface. Among of them, the wettability between water and solid surface has been studied in relation to the functional coatings on glass, mirror and other materials for controlling the surface hydrophilicity and hydrophobicity. In this context, it is well-known that TiO_2 coated materials provide multifunctional characteristics, i.e., self-cleaning and antifogging effects, based on the photo-functioal properties of TiO_2 layer.[11,12]

On the other hand, isolated tetrahedrally coordinated transition metals (single-site M moieties; M = Ti, Cr, V, Mo, etc.) containing porous siliceous materials exhibit unique catalytic and photocatalytic activities due to the well-defined structure of active sites with single-site nature.[13−18] Single-site M moieties are embedded within silica matrixes at highly dispersed state and shows different and unique catalytic performances in some cases as compared to the corresponding bulk oxides.[15−18] The additional change of powder shapes of these porous siliceous materials, i.e., construction of hierarchical and macroporous architectures, by usages of aligned polymer microspheres as template in the synthesis process led to the enhancement of their catalytic performances.[18] Moreover, in the thin film type of porous siliceous materials, the surface wettability changes to be more hydrophilic by incorporation of single-site M moieties within silica matrixes.[17,19] These films also response to irradiation of UV light and induce the changes of surface wettability to highly hydrophilic state.[17,19]

In the present work, single-site Ti embedded silica thin films with macroporous and mesoporous structures were prepared on quartz substrates by applying a conventional sol–gel dip coating method using poly(methyl methacrylate) (PMMA) microspheres and organic surfactant as templates of porous structures. We dealt with the characterization of porous structure of thin films, state of embedded Ti moieties and the positive effects of macroporous structures on the surface hydrophilicity of thin films.

2. EXPERIMENTAL SECTION

Tetraethyl orthosilicate (TEOS), tetrabutyl orthotitanate (TBOT), diethanolamine (DEA), ethanol (EtOH) and 5 N hydrochloric acid (HCl) were purchased from Nacalai Tesque Inc. Tetraethyl orthotitanate (TEOT) was obtained from Tokyo Kasei Kogyo Co., Ltd. Polyoxyethylene (20) Stearyl ether (Brij78) was purchased from Sigma-Aldrich Co. All reagents were used as received. Noncross-linked PMMA microspheres (ca. 400 nm in diameter) were supplied by Soken Chem. & Eng. Co. Ltd.

Received: May 19, 2011
Accepted: November 21, 2011
Published: November 21, 2011

   dx.doi.org/10.1021/am201265r | ACS Appl. Mater. Interfaces 2011, 3, 4561–4565

The quartz substrate (10 × 10 × 1 mm) was preliminarily washed in acetone, ethanol, and distilled water using an ultrasonic bath. After drying at 373 K for 1 h in an oven, PMMA microspheres were assembled on the clean quartz substrate by spin coating using aqueous dispersions (concentrations: 10, 20 wt.%). Single-site Ti embedded macroporous silica thin films with mesoporous frameworks (m_n-TiMSF; n describes the PMMA concentration of precoated aqueous dispersions) were prepared on a quartz substrate using two kinds of templates, i.e., preassembled PMMA microspheres and organic surfactant (Brij78) in precursor solution. A schematic illustration of the synthesis procedure is shown in Figure 1. The precursor solution

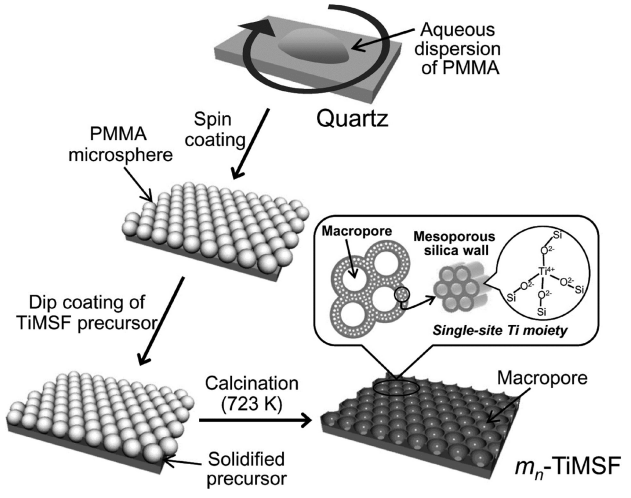

Figure 1. Schematic diagram of the procedures for preparation of single-site Ti embedded silica thin films with macroporous and mesoporous structures (m_n-TiMSF).

for thin film coating was prepared in accordance with previous literature[19−21] and used after adjustment of viscosity by the addition of ethanol. A mixture of EtOH, TEOS, TEOT, Brij78 as a structure directing agent (SDA) of mesopores and 5 N HCl was stirred in a Teflon bottle for 30 min at 298 K, followed by the addition of distilled water. The obtained mixed solution of precursors for thin film coating was transparent. The molar compositions of precursor solution were as follows: EtOH:(TEOS + TEOT):Brij78 HCl:H_2O = 20:1.0:0.05:0.015:5.0 (Si/Ti = 50). One milliliter of the thus-obtained mixture was diluted with 10 mL of EtOH and then further stirring for 30 min at same temperature. This solution was filled into the assembled PMMA template on quartz substrate during the dip-coating process (drawing rate: 10 mm min^{-1}). For comparative studies, mesoporous silica thin films (MSF) and single-site Ti embedded MSF (TiMSF) was also prepared on clean quartz substrate through the same preparation process by using Ti-free and Ti-containing precursor solution, respectively. After drying at 298 K, all samples were calcined at 723 K for 5 h (heating rate: 2.5 K min^{-1}). As a sample for comparison, TiO_2 thin film was also prepared by a conventional sol−gel method.[10] The molar ratio of sol solution was as follows: TBOT:DEA:C_2H_5OH:H_2O = 1:1:43:8. Using this sol solution, TiO_2 thin film was coated on quartz substrate by a dip-coating process (drawing rate: 10 mm/min). After drying at 298 K, all samples were calcined at 723 K for 6 h.

The XRD measurements were performed using a Rigaku Ultima IV X-ray diffractometer with Cu Kα radiation (λ = 1.5406 Å). Diffuse reflectance UV−vis spectra were recorded at 298 K with a Shimadzu UV-2450A double-beam digital spectrophotometer in air and under vacuum. For removal of adsorbed water on thin films, sample was degassed at 723 K for 1 h. The surface morphologies of thin films were observed by a field emission scanning electron microscope (FE-SEM; JEOL JSM-6500). Prior to FE-SEM analyses, sample surfaces were coated with gold/palladium using an ion sputtering device (JEOL JFC-1100). The transmission electron microscopy (TEM) image was obtained with a Hitachi Hf-2000 FE-TEM equipped with a Kevex energy-dispersive X-ray detector operated at 200 kV. TEM images were measured after peeling of prepared thin film layer from quartz substrate. Surface wettabilities of the prepared thin films were examined by contact angle measurements of a pure water droplet (ca. 1 μL) using a contact angle meter (Kyowa Interface Science Co., Ltd., DropMaster 300). An average value of water contact angle measured at three different points on the film surface was adopted. UV light irradiation was carried out with a 200 W mercury xenon lamp (San-ei Electric Co., Ltd., UVF-204S) under controlled light intensity (ca. 5 mW cm^{-2}). The light intensities at around 360 nm were measured by a UV radiometer (Topcon, UVR-2).

3. RESULTS AND DISCUSSION

Figure 2 shows FE-SEM images of prepared samples. TiMSF prepared by coating of precursor solution directly on a clean

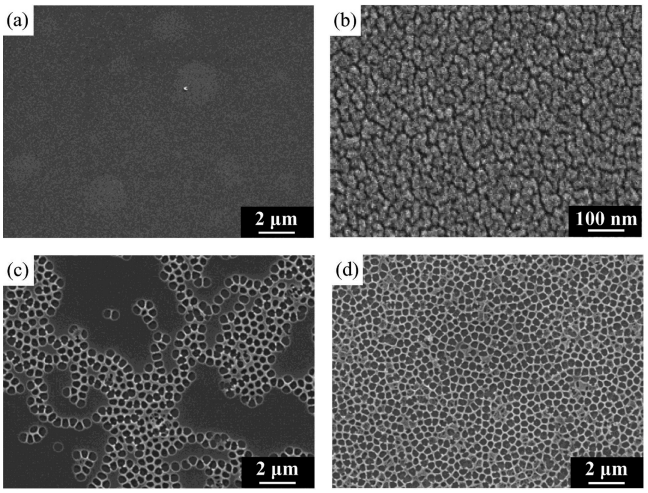

Figure 2. FE-SEM images of (a) TiMSF, (b) enlarged view of TiMSF, (c) m_{10}-TiMSF, and (d) m_{20}-TiMSF.

quartz substrate showed smooth surface without any large cracks in micrometer-scale (Figure 2a,b). Entire surface of quartz substrate was uniformly covered by TiMSF. The magnified FE-SEM image revealed that TiMSF was composed of accumulated small roundish particles in nanoscale. As shown in Figure 2(c,d), the successful construction of macropores was achieved by using assembled PMMA microspheres as template and same precursor solution for synthesis of TiMSF. As illustrated in Figure 1, the macropores were constructed through the solidification of precursor solution within the interstices of PMMA microspheres and following calcination for complete removal of templates. The formed amount of macropores depended on the PMMA concentration of the precoated aqueous dispersions. The sea-island structure of m_{10}-TiMSF was formed by the relatively sparse macropores. The dark islands consisted of TiMSF. In the case of m_{20}-TiMSF, macropores were located at overall film surface, which have scraggly and distorted circular shapes in a diameter ca. 400 nm. The film thickness of samples estimated by monitoring of cross-section FE-SEM images was ca. 200 nm, showing the good correspondences with the radius of PMMA microspheres.

XRD patterns of samples prepared by using Ti-free and Ti-containing precursor solutions were shown in Figure 3. The typical XRD peaks due to the presence of mesoporous structure were observed at around 2θ = 2.2°. The XRD peaks assignable to TiO_2 were hardly observed at higher diffraction angles,

dx.doi.org/10.1021/am201265r | ACS Appl. Mater. Interfaces 2011, 3, 4561−4565

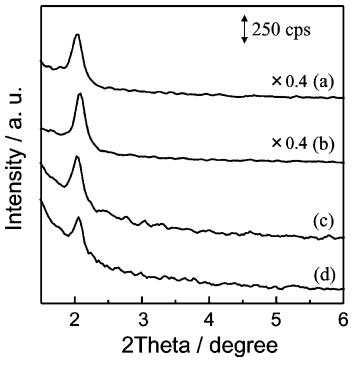

Figure 3. XRD patterns of (a) MSF, (b) TiMSF, (c) m_{10}-TiMSF, and (d) m_{20}-TiMSF.

which suggested that Ti moieties were highly dispersed in the siliceous frameworks without the formation of aggregated TiO_2 particles. Moreover, the XRD peak position of Ti-containing samples was scarcely changed irrespective of the presence of macropores, however, the peak intensity was decreased with increases in the number of macropores. TEM image of m_{20}-TiMSF was also shown in Figure S1 in the Supporting Information. This image was measured after peeling of m_{20}-TiMSF layer from quartz substrate. The existences of mesopores can be confirmed in this image, although the XRD peak of m_{20}-TiMSF was relatively small. These results suggest that the siliceous walls of macropores were composed of mesoporous structures. The reduction of the amount of TiMSF layer on quartz substrate by construction of macropores also might be influenced to some extent in the XRD peak intensity of m_n-TiMSF. Moreover, it was found that each thin film was well-fixed on quartz substrate. The changes of XRD peak intensity was scarcely observed before and after the peeling test by using commercially available tapes.

Figure 4 shows the photographic images of prepared thin films. MSF, TiMSF and m_n-TiMSF were colorless and kept

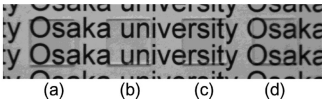

Figure 4. Photographic images of (a) MSF, (b) TiMSF, (c) m_{10}-TiMSF, and (d) m_{20}-TiMSF.

high transparency even in the existence of macroporous structure. The UV−vis absorption spectrum of each transparent thin film was shown in Figure 5. The position of the absorption edge of TiMSF and m_n-TiMSF was quite different to that of TiO_2 thin films. The absorption edge of embedded Ti moieties within silica matrixes depends on the dispersion and their local structures. The absorption band at 200−240 nm and 240−280 nm are assigned to the isolated tetrahedral Ti monomers and dimers or small oligomers, respectively.[15,22,23] These absorption bands can be assigned to the ligand to metal charge transfer (LMCT) transition from O^{2-} to Ti^{4+} of Ti moieties with tetrahedral coordination.[15,22,23] As shown in Figure 5a−d, TiMSF and m_n-TiMSF exhibited typical absorption peak at around 210 nm with small absorption in the region from 240 to 280 nm, which is clear evidence in the successful incorporation of Ti moieties within silica matrixes without the formation of aggregated species. On the other hand, TiO_2 thin films showed typical absorption corresponding to the band gap energy of

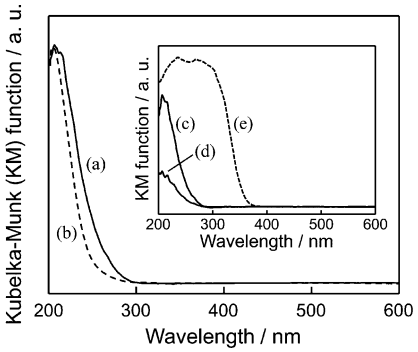

Figure 5. UV−vis absorption spectra of (a) TiMSF, (b) TiMSF after evacuation at 723 K, (c) m_{10}-TiMSF, (d) m_{20}-TiMSF and (e) TiO_2 thin films.

anatase TiO_2 (Figure 5 e). These results indicate that the isolated tetrahedral Ti monomers (single-site Ti moieties) are dominant moieties within the silica frameworks of TiMSF and m_n-TiMSF. Moreover, after evacuation at 723 K, the absorption edge of TiMSF was shifted to shorter wavelength region due to the desorption of coordinated water on Ti moieties (Figure 5a,b). This spectral change indicated that Ti moieties were located at the accessible position of molecules within mesoporous silica matrixes.

The surface wettabilities were evaluated by contact angle measurement of water droplets on each thin film surface. Figure

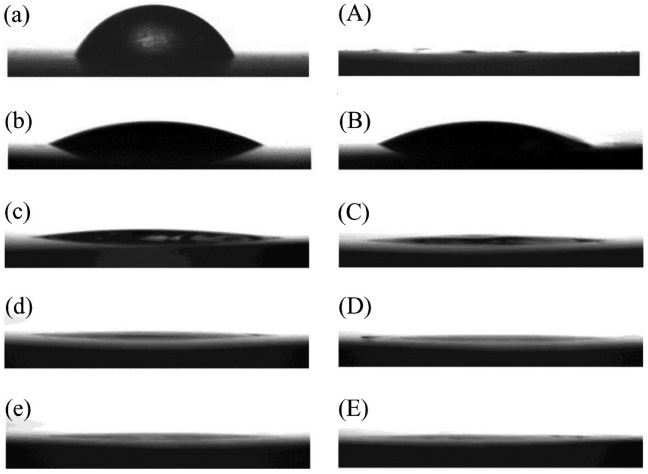

Figure 6. Photographic images of water droplets (a−e) before and (A−E) after irradiation of UV light for 3 h (Samples: (a, A) TiO_2 thin films (b, B) MSF, (c, C) TiMSF, (d, D) m_{10}-TiMSF, and (e, E) m_{20}-TiMSF).

6 shows the photographic images of water droplets on each sample before and after irradiation of UV light. The differences of surface hydrophilicity were clearly observed in these images. The water contact angle on TiO_2 thin films before irradiation of UV light (ca. 70°) is higher than that on other samples. The water contact angle on MSF was ca. 25° and scarcely changed even after irradiation of UV light (Figure 7). In the case of TiMSF and m_n-TiMSF, each sample exhibited relatively high surface hydrophilicity. The water contact angles were smaller than 10° even before irradiation of UV light and decreased with increases in the number of macropores. In response to the irradiation of UV light, single-site Ti moieties clearly induce the changes of surface hydrophilicity.[17,19] The water contact angle

dx.doi.org/10.1021/am201265r | ACS Appl. Mater. Interfaces 2011, 3, 4561−4565

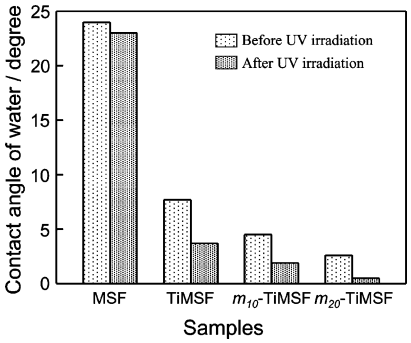

Figure 7. Contact angle of water droplet on each sample before and after UV light irradiation (irradiation time: 3 h).

apparently decreased on TiMSF and m_n-TiMSF after irradiation of UV light. Especially, the water droplet was entirely spreaded on m_{20}-TiMSF after irradiation of UV light. Meanwhile, the water contact angles on quartz substrate were scarcely changes under same experimental conditions (see Figure S2 in the Supporting Information). These results clearly showed the combination effects of macroporous and mesoporous structures for improvement of surface hydrophilicity. The differences in the compositions of film surface and the architectures directly influence the surface properties of thin films. It has been reported that the incorporation of Ti moieties for linkages with tetrahedral SiO_4 and Ti moieties is attributed to the changes in the polarity of silica matrix.[24,25] This phenomenon might be affect to the affinity of water and film surface of TiMSF, attaining the good hydrophilicity as compared to that of MSF (Ti-free thin film). Moreover, the mesoporous structure of thin films also leads to the enhancement of surface hydrophilicity owing to the capillary phenomenon.[19] The rougher surface of TiO_2 thin films exhibits a faster changing from the hydrophobic to hydrophilic state under irradiation of UV light.[26] In the case of m_n-TiMSF, the mesoporous structures are divided by macropores, leading to the increases of the fine roughness on film surface. The strong hydrophilic nature of m_{20}-TiMSF may attribute to the positive effects of above considering factors by combination of single-site Ti moieties as well as macroporous and mesoporous structures.

4. CONCLUSIONS

In summary, single-site Ti embedded highly hydrophilic porous silica thin films (m_n-TiMSF) were designed by combination of macroporous and mesoporous structures by using two kinds of templates, i.e., PMMA microspheres and organic surfactant. FE-SEM observation revealed that TiMSF was composed of accumulated small roundish particles in nanoscale. Macropores also showed scraggly and distorted circular shapes in a diameter ca. 400 nm. Tetrahedral Ti moieties embedded within silica matrix were located at the accessible position of molecules, which played crucial roles for achieving the good surface hydrophilicity. It was also found that the combination of macroporous and mesoporous structures as well as the roles of single-site Ti moieties led to a significant improvement of surface hydrophilicity even before and after irradiation of UV light.

■ ASSOCIATED CONTENT

Ⓢ Supporting Information

TEM image of m_{20}-TiMSF (Figure S1); Photographic images of water droplets on quartz substrate before and after irradiation of UV light for 3 h (Figure S2). This material is available free of charge via the Internet at http://pubs.acs.org.

■ AUTHOR INFORMATION

Corresponding Author

*E-mail: yamashita@mat.eng.osaka-u.ac.jp. Fax/Tel: +81-6-6879-7457.

■ ACKNOWLEDGMENTS

The present work was supported by Grants-in-Aid for Scientific Research (KAKENHI) from Ministry of Education, Culture, Sports, Science and Technology (20360363, 2156207 and 21760630). We also acknowledge support from the Kansai Research Foundation (KRF) for Technology Promotion. The authors appreciate Dr. Eiji Taguchi at the Research Center for Ultra-High Voltage Electron Microscopy, Osaka University, for assistance with TEM measurements.

■ REFERENCES

(1) Chen, X.; Mao, S. S. *Chem. Rev.* **2007**, *107*, 2891−2959.
(2) Xia, Y.; Yang, P.; Sun, Y.; Wu, Y.; Mayers, B.; Gates, B.; Yin, Y.; Kim, F.; Yan, H. *Adv. Mater.* **2003**, *15*, 353−389.
(3) Sun, T.; Feng, L.; Gao, X.; Jiang, L. *Acc. Chem. Res.* **2005**, *38*, 644−652.
(4) Feng, X; Jiang, L. *Adv. Mater.* **2006**, *18*, 3063−3078.
(5) Gu, Z.; Uetsuka, H.; Takahashi, K.; Nakajima, R.; Onishi, H.; Fujishima, A.; Sato, O. *Angew. Chem., Int. Ed.* **2003**, *42*, 894−897.
(6) Liu, H.; Feng, L.; Zhai, J.; Jiang, L.; Zhu, D. *Langmuir* **2004**, *20*, 5659−5661.
(7) Qian, B.; Shen, Z. *Langmuir* **2005**, *21*, 9007−9009.
(8) Stein, A; Schroden, R. C. *Curr. Opin. Solid State Mater. Sci* **2001**, *5*, 553−564.
(9) Park, S. H.; Xia, Y. *Chem. Mater.* **1998**, *10*, 1745−1747.
(10) Kamegawa, T.; Suzuki, N; Yamashita, H. *Energy. Environ. Sci.* **2011**, *4*, 1411−1416.
(11) Wang, R.; Hashimoto, K.; Fujishima, A.; Chikuni, M.; Kojima, E.; Kitamura, A.; Shimohigoshi, M.; Watanabe, T. *Nature* **1997**, *388*, 431−432.
(12) Wang, R.; Hashimoto, K.; Fujishima, A.; Chikuni, M.; Kojima, E.; Kitamura, A.; Shimohigoshi, M.; Watanabe, T. *Adv. Mater.* **1998**, *10*, 135−138.
(13) Thomas, J. M.; Raja, R.; Lewis, D. W. *Angew. Chem., Int. Ed.* **2005**, *44*, 6456−6482.
(14) Lin, W. Y.; Frei, H. *J. Am. Chem. Soc.* **2005**, *127*, 1610−1611.
(15) Ikeue, K.; Yamashita, H.; Anpo, M. *J. Phys. Chem. B* **2001**, *105*, 8350−8355.
(16) Kamegawa, T.; Morishima, J.; Matsuoka, M.; Thomas, J. M.; Anpo, M. *J. Phys. Chem. C* **2007**, *111*, 1076−1078.
(17) Yamashita, H.; Mori, K. *Chem. Lett.* **2007**, *36*, 348−353.
(18) Kamegawa, T.; Suzuki, N.; Che, M.; Yamashita, H. *Langmuir* **2011**, *27*, 2873−2879.
(19) Horiuchi, Y.; Ura, H.; Kamegawa, T.; Mori, K.; Yamashita, H. *J. Mater. Chem.* **2011**, *21*, 236−241.
(20) Nishiyama, N.; Tanaka, S.; Egashira, Y.; Oku, Y.; Ueyama, K. *Chem. Mater.* **2002**, *14*, 4229−4234.
(21) Ogawa, M. *Chem. Commun.* **1996**, 1149−1150.
(22) Marchese, L.; Maschmeyer, T.; Gianotti, E.; Coluccia, S.; Thomas, J. M. *J. Phys. Chem. B* **1997**, *101*, 8836−8838.
(23) Marchese, L.; Gianotti, E.; Dellarocca, V.; Maschmeyer, T.; Rey, F.; Coluccia, S.; Thomas, J. M. *Phys. Chem. Chem. Phys.* **1999**, *1*, 585−592.

(24) Lopez, A.; Tuilier, M. H.; Guth, J. L.; Delmotte, L.; Popa, J. M. *J. Solid State Chem.* **1993**, *102*, 480−491.
(25) Alba, M. D.; Luan, Z.; Klinowski, J. *J. Phys. Chem.* **1996**, *100*, 2178−2182.
(26) Lee, H. Y.; Park, Y. H.; Ko, K. H. *Langmuir* **2000**, *16*, 7289−7293.